# Executive Summary of the Centramatic dynamic wheel balancer fuel savings

9/3/2019

By: Steve Milliren, ESI

Introduction

Each year, more than 240 billion miles are logged by heavy semi-trucks in the United States. The freight and goods hauled by these trucks are a key component to our growing economy.

Most of these trucks and trailers are running on tires which are out of balance. The reason for this is two-fold, 1) the trucking companies prefer to keep the trucks rolling and not to take them out of service for balancing, and 2) the traditional method, **using weights attached to the wheel** for balancing a tire and wheel will not improve the overall wheel assembly balance as the brake assembly also contains imbalance which is not compensated for **using the traditional method** balancing process. It has not been deemed common practice due to these inefficiencies.

A proven and durable solution is available today from a Texas-based company known as Centramatic. Centramatic customers have reported fuel savings, as well as tire-life extension, and better road handling. While those benefits are each compelling, this report will focus only on fuel savings. It will explain in simple physics, why the savings occur, and how the well-balanced tires and wheel ends consume less fuel.

There is a category for “tire rolling resistance” in the EPA/Smart Way program, we will focus on the decreased rolling resistance of a well-balanced set of tires.

As the following charts show, the energy required to motivate a semi-truck with balanced tires is significantly less than one which has tires out of balance. As an example, a rig running at a 57.6 mph average speed will consume 2.11% less fuel than an identical rig that is running on imbalanced tires/wheel ends. Moreover, often there are temporary imbalances induced by ice, snow, mud, etc. Most consumers choose to keep their personal vehicle (car, pickup or SUV) tires balanced due to durability, safety and comfort, so it is a simple and well-known solution. The 2.11% fuel savings can be calculated and illustrated quite simply.

***Since the average long-haul driver logs about 2,170 hours per year, the energy equivalent annualized is easy to illustrate. The average truck consumes approximately 71.5 gallons per day, a 2.11% savings equals 1.5 gallons daily. That is roughly $5.00 every day. The annualized fuel savings is 406 gallons of fuel or about $1,312 per year, per truck. It is not just the savings in the cost of fuel, but the reduction of greenhouse gases. This reduction is directly proportional to the fuel savings. The emissions from 406 gallons of fuel, times the 3,522,485 Class 8 trucks on the the road equates to over 10,754,546 TONS of $CO_2$ not produced and harming our atmosphere. It also saves a noxious 294,934 lbs of $CH_4$ and 168,533,533 lbs of $NO_2$ not being released as well.**

But how does the Centramatic Balancing System do this? In short, **Less Rolling Resistance**.

The animations from ESI's SimulationX product show a side-by-side physics-based video of a balanced tire, verse an unbalanced tire. Clearly, the **Tire's Footprint** (tire in contact with road) is oscillating on the out of balanced tire, and the balanced tire has a constant **Foot Print**. The energy waste is partially heat from the sidewalls flexing, but also from the suspension dampeners heating up as they slow down the bouncing effect. Additionally, the **Tire Footprint** of an extremely out of balance tire can literally cycle between zero square inches of contact, to more than 128 square inches of contact as the masses push the tire back down to the road.

As the **Tire's Footprint** grows, so does the bulge in the forward section of the tire. The effect is the same as climbing a slight hill and even more energy is wasted.

The predictions that ESI had made match approximately with the fuel savings reported for years by Centramatic customers. There are other applications of the dynamic wheel balancer for RV's, pickup trucks, and even motorcycles.

After reading and understanding the attached technical report, it will become clear that rolling resistance is decreased using the dynamic wheel balancer. For this reason, the EPA/Smart Way Program would be serving its taxpayers well by adding a dynamic wheel balancing category as a section of Low Rolling Resistance.

* Figures based upon Fuel at $3.25/Gallon, 125,000 miles per year, 6.5 miles per gallon.
* For the purposes of this study, we will refer to tires, wheels, drums and all the rotating mass as wheel ends.

# Energy Savings Using Centramatic Wheel Balancers

Purna Musunuru
*ESI North America*

## 1. Introduction

With the ever-increasing demand for reduction of greenhouse gas emissions, the current need for fuel efficient transport is more than ever. This is especially true in case of light-duty vehicles (cars, small trucks, vans, SUVs, motorcycles), commercial and freight trucks both of which account for about 78% of the total energy use in the transportation sector [1]. Researchers and companies are continuously looking for ways to improve fuel efficiency. Tire imbalance is one such area where there is loss of energy when a tire is not properly balanced. This study focuses on the effect of using *Centramatic* wheel balancers on the overall energy consumption, specifically in class 8 trucks where tires are rarely in balance.

## 2. Modeling Methodology

A physical object-oriented modeling approach was followed for this project. Object-oriented (or network based) modeling is the natural way to describe any kind of physical behavior in simulation models. This modeling concept is shown in figure 1. Physical network models are formed of elements which are interconnected with each other by connections, also called as nodes. The physical relationships are then formulated in terms of potential and flow quantities. The potential quantities reside inside the connection and are identical for all the element connectors connected to it. Examples of such potential quantities are displacements, spends and accelerations in mechanics, pressures in fluids, voltages in electronics, temperatures in thermal models.

The flow quantities are the quantities for which certain balance equations must be fulfilled. For example, the forces or torques (depending on linear or rotational mechanics) at the connections in mechanics models must balance to zero.

Elements define the relationships between the potential quantities at their connectors and their internal flow quantities. For example, a translational mechanical spring relates internal force $F$ and the displacement difference $dx$ between its connectors via the stiffness parameter $k$ by an equation $F = k*dx$.

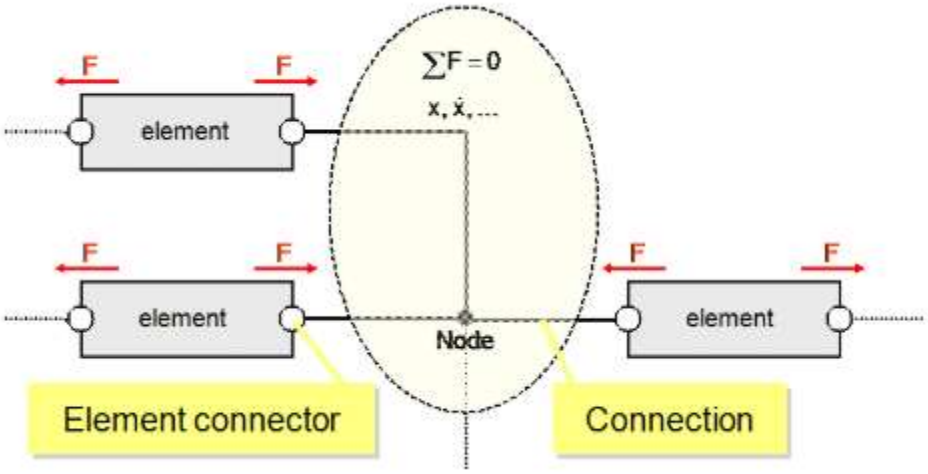


*Figure 1: Modeling Concept*

The models described in the following sections follow a similar methodology (elements and connections).

### 2.1 Drive and Trailer Axle Setup

This section discusses the quarter-truck setup of the tandem drive axle. Since the configuration for the drive and trailer axles is similar, the same setup is extended to the trailer axle. Figure 2 below gives an overview of the full setup and figures 3 and 4 show zoomed versions of some key elements within the setup. The elements in figure 3 are discussed from here on.
The *posDrive* element models a rigid massles link with zero degrees of freedom. This is used to fix the wheel center position as reference.
The *dofLongDrive* element is a prismatic joint representing one translational degree of freedom along a selectable axis (the longitudinal direction in this case). This prismatic joint generates two potential state variables i.e. the relative displacement and relative velocty along the longitudinal direction. Additionally, this element also gives the flexibility to model the friction and also specify actuation (either a force or a displacement or a velocty) through the linear mechanical connectors along the direction of choice.

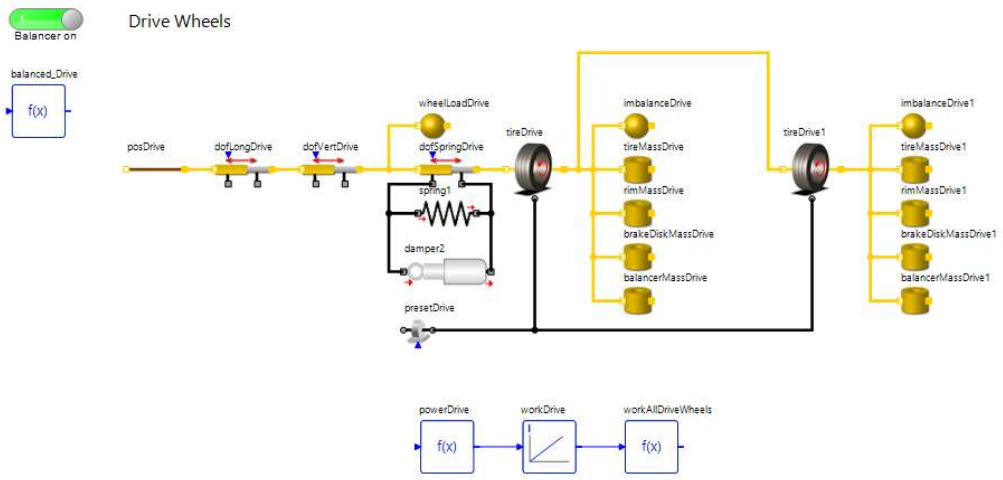


*Figure 2: Drive axle full setup*

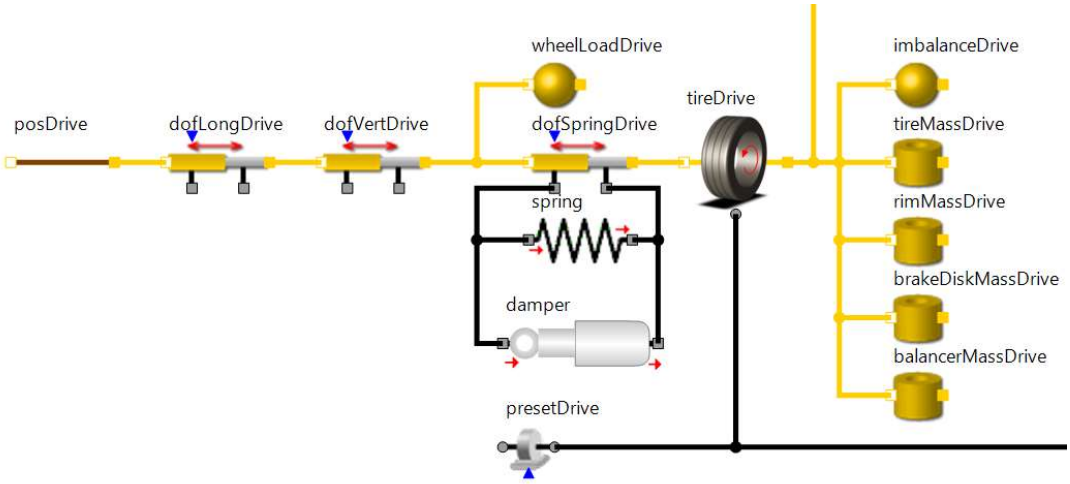


*Figure 3: Drive axle – tire & wheel assembly, shock absorber setup*

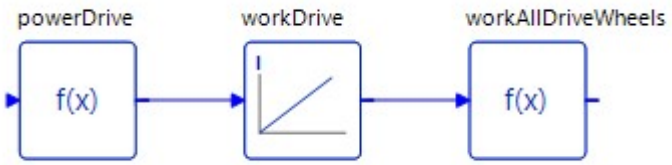


*Figure 4: Drive axle – work done computation*

The *dofVertDrive* element represents the same physical behavior as the *dofLongDrive.* The degree of freedom in this case is set to the vertical direction.

The *wheelLoadDrive* element is a rigid body with 6 DOF, accounting for the quarter of the total load on the tandem drive axle. Cosnidering a truck with a GVW of 80,000 lbs, the distribution of

loads on the steer, drive and trailer axles are 12,000, 34,000 and 34,000 lbs respectively. Since we are only considering a quarter of drive axle in this set-up, the mass of the wheelLoadDrive element is set to 8,500 lbs (34,000/4).
The flexibility due to the shock absorber in the vertical direction is then defined through the *dofSpringDrive* element. As seen, the mechanical conectors are actuated through *spring* and *damper* elements.

### 2.1.1 Spring Element

The *spring* element represents a translational stiffness describing the elastic behavior.
The internal force of the spring is computed from the following expression
Internal force $F_i = k * dx$
Where *k* is the stiffness of the spring, *dx* is the displacement difference which is the difference between the current displacements of the connections.
Displacement difference $dx = ctr1.x - ctr2.x$
To parameterize the stiffness of the spring, a full load compression of 4 inches is assumed (which is typical for shock absorbers for the 18-wheeler heavy duty trucks).
In addition to the intenal force and displacement difference, the velocty difference and the change of potential energy are also computed within the spring element based on the following relations
Velocity difference $dv = ctr1.v - ctr2.v$
Change of potential energy $P_p = F_i * dv$

### 2.1.2 Damper Element

The *damper* element models the non-linear behavior described through a characteristic curve of damping coefficient. Similar to the spring element, the displacement and velocity difference are computed based on the potential varibles from the connectors
Displacement difference $dx = ctr1.x - ctr2.x$
Velocity difference $dv = ctr1.v - ctr2.v$
The inner damping force is then computed based on the following relation
Damping force $F_i = dv * bCurve(dv)$
Where *bCurve(dv)* is the non-linear damping curve i.e. damping constant defined as a function of velocity difference. This non-linear damping curve is parameterized based on the literature [2] as shown in figure 5.

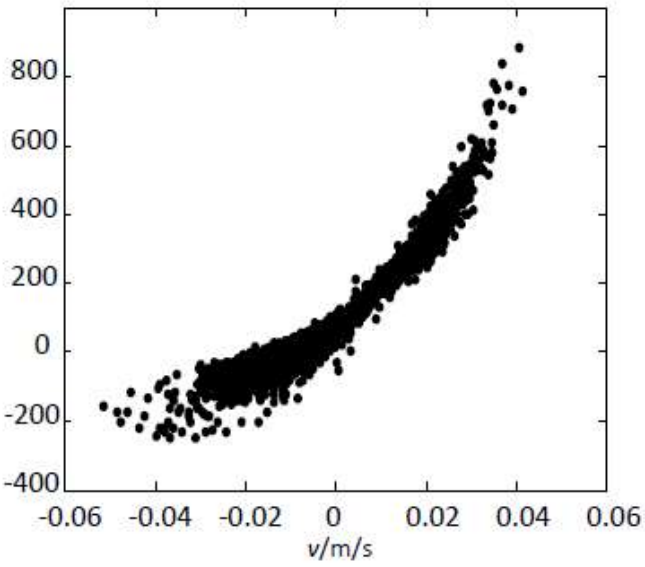


*Figure 5: Non-linear shock absorber damping curve*

For region outside of $\pm\ 0.06\ m/s$, a linear extrapolation technique is implemented. Finally, the power loss in the damper element is computed as follows

Power loss $P_l = F_i * dv$

### 2.1.3 Tire Model

The *tireDrive* element models a pneumatic tire which is regarded as a sping and damper element between hub and road surface. This element does not consider any inertia and hence rigid bodies need to be connected to model the rim, tire, brake disk inertias.

Figure 6 illustrates different coordinate systems of the tire. This description is consistent with the Tyre Data Exchange (TYDEX) format [3].

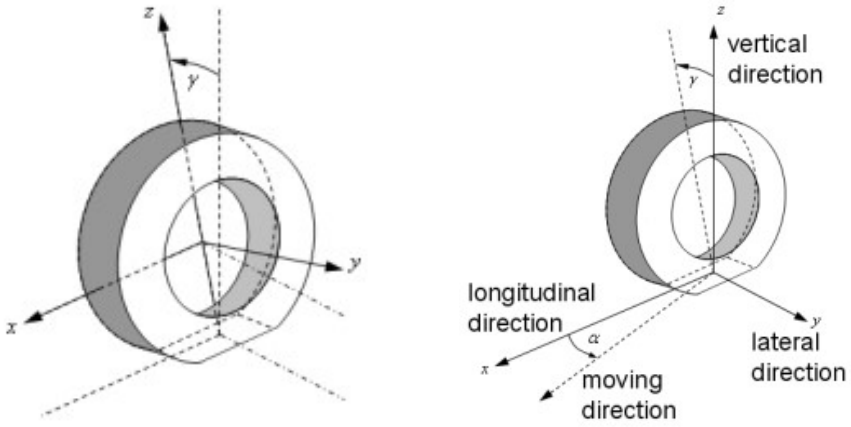


*Figure 6: Tire co-ordinate systems in TYDEX format*

The X-axis of the TYDEX center axis coordinate system is in the central plane of the wheel and is parallel to the ground. The driving or braking torque acts around the axis of wheel rotation, i.e. the Y-axis of the TYDEX center axis coordinate system as seen in figure 6.
Depending on the nominal wheel load, a contact area (tread shuffle) emerges between road and tire. Due to the pressure distribution along the tread shuffle, a friction force is then generated if there is a difference velocity between road and tire. This force distribution is summed up as vectors of tire forces and tire torques acting at the contact point between road and tire (wheel intersection point). This contact point is the origin of the TYDEX wheel axis coordinate system as seen in figure 6. The X-axis of the TYDEX wheel axis coordinate system is parallel to the X-axis of the TYDEX center axis coordinate system. The Y-axis is given by the projection of the axis of wheel rotation onto the ground. The Z-axis is normal to the ground and points upwards.
The side slip angle *alpha* is defined as the angle between moving and longitudinal direction. The camber angle *gamma* is the angle between the Z-axes of the TYDEX wheel and center axis coordinate systems.

The resulting tire forces and torques then depend on the slip values in longitudinal and lateral direction. The slip value *lambda* increases with increasing driving torque and there is a non-linear relationship between the friction behavior and the tire force as seen in figure 7. For small slip values, i.e. when the tire sticks to the road, the force increases linearly. If the slip value exceeds a certain threshold, the tire then starts to slip. The final force of the sliding friction $F_{Slip}$ is less than the maximum force $F_{Max}$ of the static friction as the slip value approaches 1.

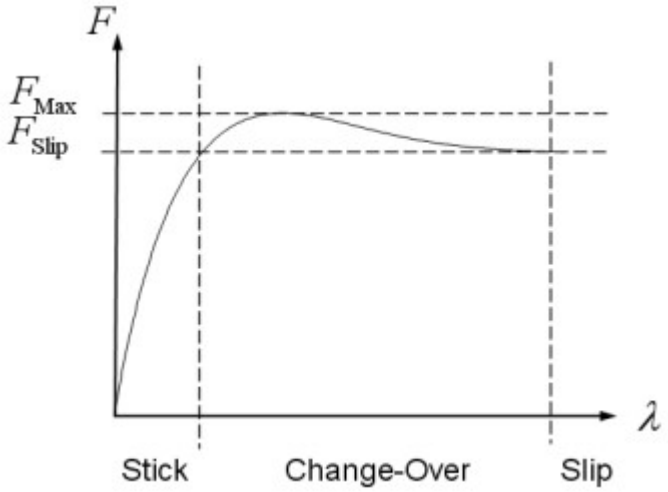


*Figure 7: Tire slip characteristic curve*

Based on this, the tire forces and torques are then calculated using the semi-empirical *Pacejka Tire Model* [4].
It uses only one formula with different sets of parameters for the each computation, i.e. the longitudinal force, the lateral force and the self-aligning torque. The basic equation of this magic formula is

$$f_{Magic}(x) = D\sin\big(C\arctan\big(B(1-E)(x+S_H) + E\arctan\big(B(x+S_H)\big)\big)\big) + S_V$$

with stiffness factor *B*, shape factor *C*, peak value *D*, curvature factor *E*, horizontal shift *SH*, and vertical shift *SV*.

**Slip Calculation**

The longitudinal slip velocity *vsx* is defined as difference between peripheral speed, i.e. the product of the effective rolling radius *re* and the relative angular velocity *omRel*, and the longitudinal velocity *vx*.

$$V_{sx} = r_e\, W_{Rel} - v_x$$

The lateral slip velocity *vsy* equals the lateral velocity *vy*.

$$v_{sy} = v_y$$

The total slip velocity *vst* is the absolute value of the slip velocity vector .

$$v_s = \left(v_{sx}\; v_{sy}\right)^T$$

$$v_{st} = \sqrt{(v_{sx}^2 + v_{sy}^2)}$$

The slipping angle *alpha_lambda* are determined by formulae

$$\cos(\alpha_\lambda) = \frac{v_{sx}}{v_{st}}$$

$$\sin(\alpha_\lambda) = \frac{-v_{sy}}{v_{st}}$$

The longitudinal slip *lambda_x*, the lateral slip *lambda_y* and the total slip *lambda_t* can be obtained by formulae

$$\lambda_x = -\frac{v_{sx}}{r_e\, W_{Rel}}$$

$$\lambda_y = -\frac{v_{sy}}{r_e\, W_{Rel}}$$

$$\lambda_t = -\frac{v_{st}}{r_e\, W_{Rel}}$$

**Tire Forces Calculation**

The longitudinal tire force *Fx* can be calculated by means of the eight coefficients *CxP* of the magic formula.

The variable *Xx* can be interpreted as an equivalent longitudinal slip.

$$X_x = -100\,\frac{\lambda_t}{1+\lambda_t}$$

The variable *Bx* can be interpreted as stiffness factor of the longitudinal force over slip characteristic curve.

$$B_x = \frac{C_{xP3}\,F_z^2 + C_{xP}\;\;F_z}{C_x\;D_x\,\exp(C_{xP}\;\;F_z)}$$

The shape factor Cx is set to 1.65 for longitudinal force calculation and can not be changed.

$$C_x = 1.65$$

The variable *Dx* can be regarded as peak value of the longitudinal force over slip characteristic curve.

$$D_x = C_{xP1}\,F_z^2 + C_{xP2}\,F_z$$

The variable *Ex* corresponds to the curvature of the longitudinal force over slip characteristic curve.

$$E_x = C_{xP}\;\;F_z^2 + C_{xP}\;\;F_z + C_{xP8}$$

There is neither a horizontal nor a vertical shift of the longitudinal force over slip characteristic curve, hence the shift parameters *SHx* and *SVx* vanish.

$$S_{Hx} = 0$$

$$S_{Vx} = 0$$

Once all parameters are calculated the magic formula can be applied to finally get the longitudinal tire force.

$$Y_x = D_x \sin\big(C_x \arctan\big(B_x(1-E_x)(X_x+S_{Hx}) + E_x \arctan\big(B_x(X_x+S_{Hx})\big)\big)\big) + S_{Vx}$$

$$F_x = Y_x \cos(\alpha_\lambda)$$

The lateral tire force *Fy* is calculated in a similar fashion as *Fx* as follows

$$X_y = -\frac{180}{\pi}\arctan(\lambda_t)$$

$$B_y = \frac{C_{yP3}\sin\left(C_{yP4}\arctan\left(C_{yP5}\,F_z\right)\right)}{C_y D_y}\left(1 - C_{yP12}\,\gamma\right)$$

$$C_y = 1.3$$

$$D_y = C_{yP1}\,F_z^2 + C_{yP2}F_z$$

$$E_y = \frac{C_{yP6}F_z^2 + C_{yP7}F_z + C_{yP8}}{1 - C_{yP13}\,\gamma}$$

$$S_{Hy} = C_{yP9}\,\gamma$$

$$S_{Vy} = \left(C_{yP10}F_z^2 + C_{yP11}F_z\right)\gamma$$

$$Y_y = D_y \sin\left(C_y \arctan\left(B_y\left(1 - E_y\right)\left(X_y + S_{Hy}\right) + E_y \arctan\left(B_y\left(X_y + S_{Hy}\right)\right)\right)\right) + S_{Vy}$$

$$F_y = Y_y \sin(\alpha_\lambda)$$

**Self-Aligning Torque**

The self-aligning torque *Tz* is similarly calculated similar to the lateral and longitudinal forces. The computation of coefficients *Xn, Bn, Cn, Dn, En, $S_{Hn}$, $S_{Vn}$* is done in a similar way. Then *Yn* and *Tz* are calculated as follows

$$Y_n = D_n \sin\left(C_n \arctan\left(B_n(1 - E_n)(X_n + S_{Hn}) + E_n \arctan\left(B_n\,(X_n + S_{Hn})\right)\right)\right) + S_{Vn}$$

$$T_z = -Y_n \sin(\alpha_\lambda)$$

**Tire Dynamics**

A linear three-dimensional spring and damper system with stiffness $k = (k_x\ k_y\ k_z)^T$ and damping coefficient $b = (b_x\ b_y\ b_z)^T$ is introduced to incorporate the first order tire dynamics. The vertical force *Fz* is then calculated by the following spring-damper equation along the Z-direction of the wheel axis coordinate system

$$F_z = k_z\,d_{xz} + b_z\,d_{vz}$$

where *dx* is the three-dimensional vector of tire deformation and *dv* is the vector of deformation velocity

**Effective Rolling Radius**

The calculation of effective rolling radius *re* follows a magic formula approach

$$r_e = r - \frac{F_{zN}}{k_z}\left(C_{r2}\arctan\left(\frac{C_{r1}\, d_{xz}\, k_z}{F_{zN}}\right) + \frac{C_{r3}\, d_{xz}\, k_z}{F_{zN}}\right)$$

Figure shows the dependency of the effective rolling radius *re* on the vertical deformation *dxz*

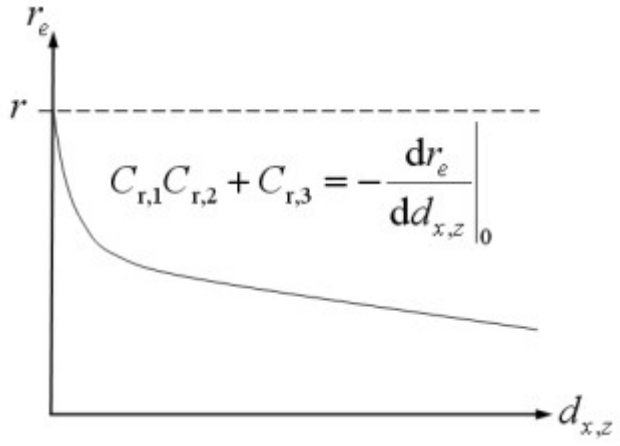


*Figure 8: Effective rolling radius characteristic curve*

The three coefficients of the radius characteristics *Cr* can be interpreted as low load stiffness, peak value and high load stiffness of the effective rolling radius.

**Overturning Torque**

The overturning torque *Tx* is approximated according to reference by formula

$$T_x = -\frac{1}{12}\, w^2 k_z \gamma$$

where *w* is the width of the unloaded tire.

**Rolling Resistance Torque**

The rolling resistance torque *Ty* is calculated as follows

$$T_y = -\mu_r\, r\, F_z \begin{cases} sign(v_x) & if\ |v_x| > v_e \\ \dfrac{v_x}{v_e} & if\ |v_x| \le v_e \end{cases}$$

Where *Ve* is a small threshold longitudinal velocity to make sure the torque curve is continuous and $\mu r$ is the rolling resistance coefficient.

**Parameterization**

The following parameters are input into the corresponding elements

Rolling Resistance $\mu_r$ = 0.005 [5]

**Tire elastic properties** [6][7]

Tire Vertical Stiffness *k[3]* = 500 kN/m

Tire Vertical Damping *b [3]* = 261 Ns/m

**Tire Geometry** [8]

Wheel Radius *rW* = 21.95 in

Tire Width *wT* = 11 in

**Masses**

The maases of the elements present in the tire assembly are captured through the *tireMassDrive, rimMassDrive, brakeDiscMassDrive* elements who values are 125.7 lbs, 51 lbs, 22 lbs respectively [8][9].

In addition, an imbalance mass of 8 oz for the tire and a miscallaneous imbalance (from drive shaft, brake disc wear etc.) of 2 oz are captured at the circumference of each tire.

In the presence of a balancer all the imbalance mass and an additional 11 lbs (*Centramatic* balancer for drive and trailer axles) is captured at the center of the wheel.

### 2.1.4 Work Done Computation

The *presetDrive* element in figure 3 is used to set an rpm as a boundary condition to the tire model. This element gives out the power required to run the truck at that particular speed. This power is read into the *powerDrive* element in figure 4 which is then integrated in the *workDrive* element to compute the total work done. This work done is then multiplied by 4 inside the work *AllDriveWheels* to capture the work done by all the drive wheels. The same computation is extended to the trailer and steer axles to compute the total work done by the truck. The total work done is then computed with and without the balancers and the resulting energy savings are computed as follows

Wo = Work done without the balancers

Wn = Work done with the balancers

$$Energy\ Savings\ (\%) = \frac{(W_o - W_n) * 100}{W_o}$$

## 2.2 Steer Axle Setup

The steer axle has a similar setup to the drive/trailer axle as seen in figure but with the following changes

- An additional air drag resistance on the truck captured as follows
    - Drag Force $F_d = 0.5 * C_d * \rho * A * v^2$

      Where $C_d$ is the drag coefficient (a value of 0.51 assumed), $A$ is the frontal area (75.3 sq ft i.e. 7 $m^2$) assumed, $\rho$ is the air density, $v$ is the relative truck speed.
    - Total drag force is then divided by 2 to account for the full steer axle
- Effective axle load in the *wheelLoadSteer* element set to 12,000/2 lbs
- The damping coefficient in the *damper3* element is set to 0.7 times the damping coefficient of the damper in the drive/trailer axle to account for lesser load per one side of the axle (34000/4 lbs vs 12,000/2 lbs)
- Tire and rim geometry, masses based on [9] [10]
- Balancer mass of 6 lbs (*Centramatic* balancer for steer axles)
- Total work done multiplied by 2 for 2 steer wheels

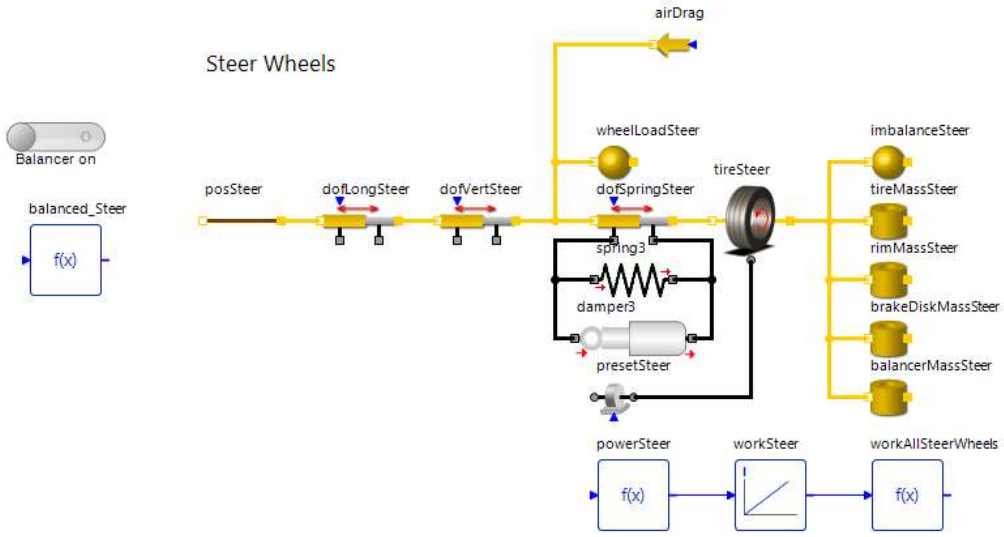

*Figure 9: Steer axle setup*

## 3. Scenario Setup and Results

The test scenario is setup in the following way

- Truck runs at a constant speed of 57.5 mph for 2 hours
- A damping degradation of 30% assumed
- The work done at all the drive, trailer and steer wheels is added and total work done is computed in both the scenarios

Figures 10 and 11 show the velocity difference (dv) profile across the shock absorber without and with the balancer respectively with an imbalance of 8 oz. As seen from the figures, the presence of balancer suppresses all the oscillations resulting in energy savings. The energy savings, which is computed based on the section 2.1.4 is shown in the table 1

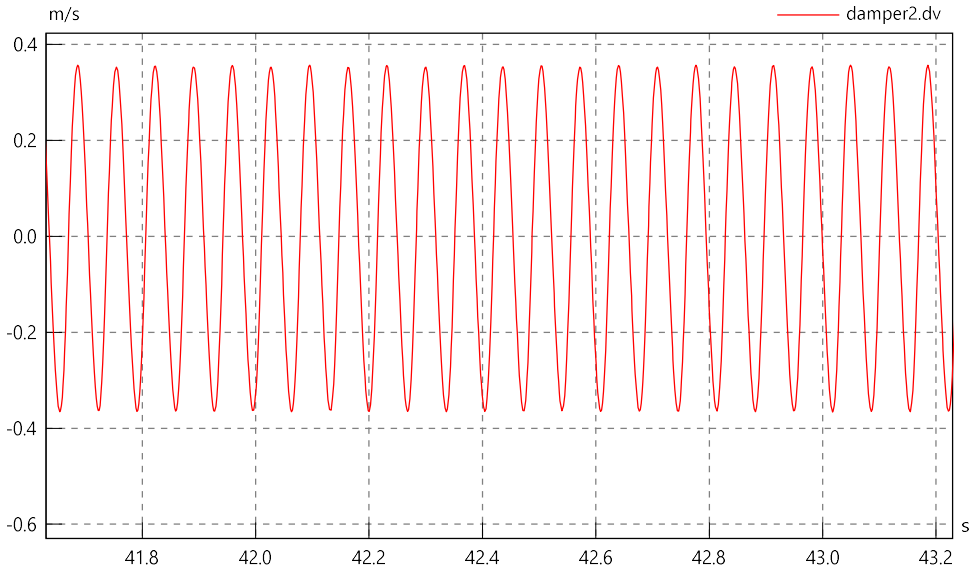


*Figure 10: Velocity difference across the shock absorber – no balancer*

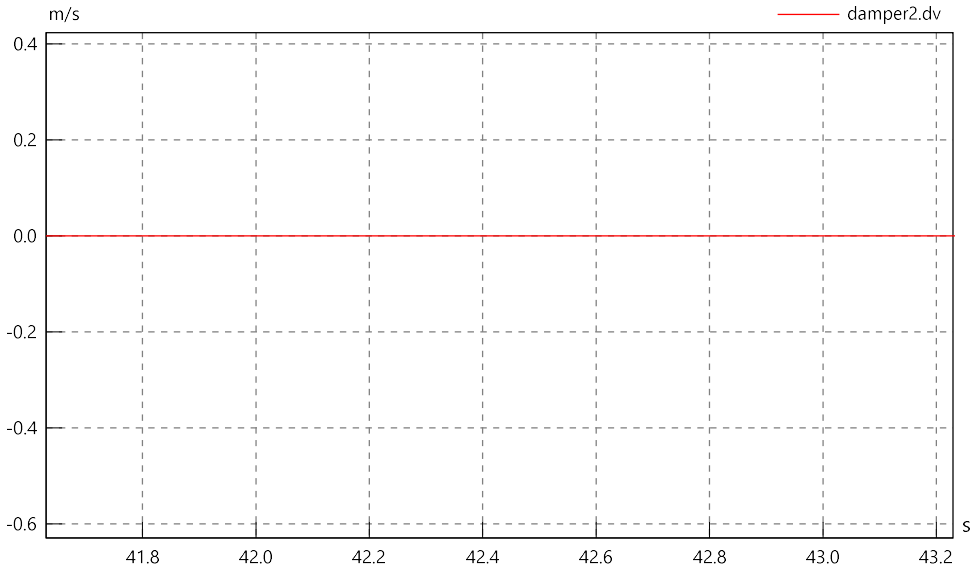


*Figure 11: Velocity difference across the shock absorber – with balancer*

| **Energy Savings** | | |
|---|---|---|
| Average imbalance per tire (oz) | 8 | |
| Miscellaneous imbalance per tire (oz) | 2 | |
| Work done without balancers Wo (kWh) | **170.833** | **2.11%** |
| Work done with balancers Wn (kWh) | **167.222** | |

*Table 1: Energy savings calculation*

## 4. Summary

A network-based simulation approach was followed to determine the fuel savings in the presence of *Centramatic* wheel balancers. As seen from the results, *Centramatic* wheel balancers offers fuel savings of about 2.11%. These fuel savings can be completely attributed to the presence of wheel balancers as the model gives the flexibility of maintaining exact same physical conditions when performing tests with and without the wheel balancers. In addition, the balancers also offer much quieter ride as seen from the vibration reduction. This would also lead to much longer tire life i.e. less tread wear thereby resulting in an even increased cost savings.

## 5. References

[1]https://www.eia.gov/energyexplained/index.php?page=us_energy_transportation#tab2
[2] Yongjie Lu, Shaohua Li and Na Chen, Research on Damping Characteristics of Shock Absorber for Heavy Vehicle, Institute of Mechanical Engineering, Shijiazhuang Tiedao University, Shijiazhuang, China
[3] J.J.M. van Oosten, H.-J. Unrau, A. Riedel, and E. Bakker: Standardization in Tire Modeling and Tire Testing - TYDEX Workgroup, TIME Project, Tire Science and Technology, Volume 27, Issue 3, pp. 188-202, July 1999.
[4] E. Bakker, L. Nyborg, and H.B. Pacejka: Tire Modelling for Use in Vehicle Dynamics Studies. Society of Automotive Engineers, January 1987.
[5] Germana Paterlini, Rolling Resistance Validation, Minnesota Department of Transportation, Principal Investigator, FuelMiner, Inc.
[6]https://tigerprints.clemson.edu/cgi/viewcontent.cgi?article=1123&context=all_theses
[7] https://ir.library.dc-uoit.ca/bitstream/10155/523/1/Reid_Adam_C.pdf
[8] https://www.otrusa.com/product/11r24-5-h-bf-goodrich-dr444-drive/
[9] https://www.arconic.com/alcoawheels/north-america/en/products/product.asp?prod_id=4591
[10] https://www.otrusa.com/product/11r24-5-h-bf-goodrich-st244-steer/
[11] www.simulationx.com

## 6. ESI Group: Company History and Credibility

ESI (Engineering System International) was founded in France in 1973 by Alain de Rouvray, current Chairman and President, and three other Berkeley PhDs (Jacques Dubois, Iraj Farhooman, Eberhard Haug). The company initially operated as a consulting company. ESI gradually developed sophisticated simulation techniques based on Finite Element Analysis (FEA) and acquired a broad understanding of industrial processes and needs.
Following a strong demand from German automotive companies as they started to implement the very first crash and safety regulations, ESI opened a subsidiary in Germany (ESI GmbH) in 1979. In 1985, ESI teamed up with a German consortium led by Volkswagen to become the first company to develop simulation software analyzing the severe deformations inflicted on a car because of a crash. This was the first step towards the development of ESI's flagship product PAMCRASH, now part of ESI Virtual Performance Solution.
To expand the company's software branch for many more industrial applications, the Group carried out a share capital increase in 1991 with the California-based venture capital firm Burr Egan Deleage, which invested 3 million US Dollars. ESI then developed a unique set of software

tools to speed up the manufacturing and testing process of industrial products, while improving their design. These tools today fall under ESI's Virtual Manufacturing tool chain. To further reinforce this tool chain and build expertise in metal stamping solution, ESI acquired *Dynamic Software,* editor of Optris virtual press software in 1999.
With its Initial Public Offering (IPO) on July 6th, 2000, ESI Group was successfully listed in Eurolist Compartment C of Euronext Paris stock market and raised around 30 million Euros. In the same year ESI Group successfully obtained its first ISO 9001 certification. With the mission to deliver Virtual Prototyping solutions that improve industrial product development and a vision to be the leader in that, ESI expanded into multi-domain simulation (NVH, Durability, Vibro-Acoustics, Comfort) in 2001 in addition to creating subsidiaries in Czech Republic, Spain, UK, India, China, Italy, Brazil and Tunisia.
In 2011, ESI entered the virtual reality segment by acquiring *IC.IDO GmbH*, a leading European vendor of Virtual Reality solutions. Embracing the open source, ESI then acquired *OpenCFD* the makers of OpenFOAM. ESI then continued its series of acquisitions with *ITI GmbH*, a global leader in the realistic simulation of mechatronic and multi-domain systems and its software *SimulationX* and *Mineset Inc*., a data analytics and machine learning specialist. At the end of 2016, ESI announced the transfer of its shares from compartment C to compartment B of Euronext Paris. ESI then created a Hybrid Twin™ solution leveraging simulation, physics and data analytics, enabling manufacturers to deliver smarter and connected products, predict product performance, and anticipate maintenance needs.
Today, ESI employs more than 1200 Virtual Prototyping specialists worldwide. Headquartered in Paris (France), the company and its global network of agents provide sales and technical support to customers in more than 40 countries. ESI has built a worldwide network of experts in each industrial domain, allowing the company to be close to its clients and to meet their needs.

## SimulationX Success Stories

### 1) Automotive

#### a) BMW Group

*With SimulationX, BMW is now able to model, simulate and analyze powertrains comprehensively throughout the whole design process – in addition, engineers benefit a great deal from its ease of use.*
*The Simulation results achieved with SimulationX are in line with the data BMW measures. Consequently, the company applies this simulation method to more and more areas of the development process.*

#### b) ZF Group

*By using SimulationX, we achieve reliable simulation models of powertrains. With these models, we are able to optimize the NVH functionality of our products.*

#### c) Honda Research Institute

*SimulationX is an excellent solution to integrate both automotive and building simulations for smart energy management on one single platform.*

## 2) Energy

### a) Eickhoff

*SimulationX allows us to optimize the wind turbine's gearbox and drivetrain components to reduce dynamic loads, which in turn increases reliability and availability of the wind turbine.*

### b) Veolia

*Our partnership with ITI (SimulationX) paid off very well as it enabled us to develop and study simulation scenarios in SimulationX tailored exactly to our needs*

## 3) Industrial Machinery

### a) Karl Mayer

*Our machines are made up of mechatronic systems which require virtual modeling. SimulationX is the innovative interdisciplinary solver we could use for all such kinds of mechatronic product development*

## 4) Marine

### a) Bureau Veritas

*We chose SimulationX not only because of its advantage as a modular solution but also because it offers the benefits of an open multi-domain platform that does not just focus on one use such as analyzing torsional vibrations. We also plan to use it to manage energy efficiency in ships.*

## 5) Mining

### a) TAKRAF

*SimulationX allows us to quickly and safely calculate dynamic effects in challenging belt conveyer projects.*

## 6) Mobile Machinery

### a) ABB

*SimulationX allows us to systematically analyze loads and optimize capacities of electromechanical machinery*